Journal of ELECTRONIC MATERIALS, Vol. 46, No. 10, 2017
DOI: 10.1007/s11664-017-5625-3

Voltammetric Sensor Based on Fe-doped ZnO and TiO_2 Nanostructures-modified Carbon-paste Electrode for Determination of Levodopa

AZAM ANARAKI FIROOZ,[1,2] BAHRAM HOSSEINI NIA,[1] JAVAD BEHESHTIAN,[1] and MASOUMEH GHALKHANI[1]

1.—Department of Chemistry, Faculty of Science, Shahid Rajaee Teacher Training University, P. O. Box 167855-163, Tehran, Iran. 2.—e-mail: a.anaraki@srttu.edu

In this study, undoped and 1 wt.% Fe-doped with ZnO, and TiO_2 nanostructures were synthesized by a simple hydrothermal method without using templates. The influence of the Fe dopant on structural, optical and electrochemical response was studied by x-ray diffraction, scanning electron microscopy, UV–Vis spectra, photoluminescence spectra and electrochemical characterization system. The electrochemical response of the carbon paste electrode modified with synthesized nanostructures (undoped ZnO and TiO_2 as well as doped with Fe ions) toward levodopa (L-Dopa) was studied. Cyclic voltammetry using provided modified electrodes showed electro-catalytic properties for electro-oxidation of L-Dopa and a significant reduction was observed in the anodic overvoltage compared to the bare electrode. The results indicated the presence of the sufficient dopants. The best response was obtained in terms of the current enhancement, overvoltage reduction, and reversibility improvement of the L-Dopa oxidation reaction under experimental conditions by the modified electrode with TiO_2 nanoparticles doped with Fe ions.

Key words: ZnO, TiO_2, Fe-doped, voltammetric sensor, levodopa

INTRODUCTION

Levodopa (L-Dopa) is an amino acid that is made from the essential amino acids in the brain and mammalian body, and is found in certain kinds of herbs and food. It is made by biosynthesis from the amino acid L-tyrosine (Fig. 1). L-Dopa is used as a therapeutic drug in the clinical treatment of Parkinson's disease and dopamine-responsive dystonia which compensates for a deficiency of dopamine in the organism and decreases the symptoms of Parkinson's disease.[1–3] Various chemically modified carbon-paste electrodes have been widely used in electrochemical applications as sensitive and selective electrodes for the determination of L-Dopa.[4,5]

Among different modifiers, nanometal oxide materials have attracted a great deal of attention due to their unique properties, such as large surface area, high thermal and chemical stability, tunable porosity and biocompatibility.[6–9] These nanometal oxide materials show interesting morphological, functional, and catalytic properties. Thus, they can provide suitable microenvironments for the immobilization of biomolecules and enhancing of biosensing characteristics with higher electron-transfer kinetics and high adsorption capability.[10]

Nanostructures-modified electrodes have been adopted as a promising way to facilitate the direct electron transfer of biomolecules. These nanostructures include, for example, carbon-paste electrodes (CPE) modified with a mixture of metal oxide nanoparticles.[10–13] Among metal oxides, zinc oxide (ZnO) and titanium dioxide (TiO_2) nanostructures are preferred for the development of sensors and

(Received March 13, 2017; accepted May 25, 2017; published online June 9, 2017)

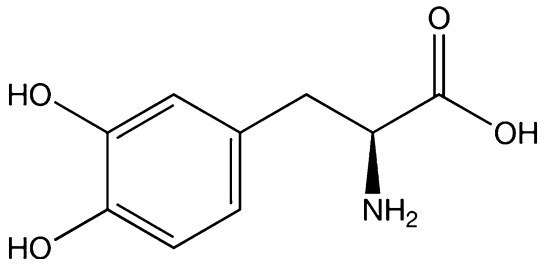

Fig. 1. Structure of levodopa.

biosensors for clinical diagnostics due to their wide band gap, large excitation binding energy, non-toxicity, and high electron communication features.[14–19]

In this work, we synthesized ZnO and TiO_2 nanostructures (undoped and also doped with 1 wt.% Fe nanoparticles) by a hydrothermal method at low temperature. We studied the Fe dopant effect on the morphology, crystal structure, band gap, and crystal defects, and also described the preparation and application of these nanostructures as new sensors for the investigation of the electrochemical behaviour of L-Dopa.

EXPERIMENTAL

Reagent and Chemicals

Graphite fine powder, paraffin oil and all other chemicals were purchased from Merck. All the electrochemical measurements were performed at 25 ± 1°C with a three-electrode assembly, including an Ag/AgCl electrode as the reference electrode and a platinum wire as the counter electrode. The working electrode was either an unmodified CPE or ZnO, TiO_2, Fe-doped ZnO and Fe-doped TiO_2 modified CPE (FeZnO/CPE) and ($FeTiO_2$/CPE).

A 100-μM L-Dopa solution was prepared daily by dissolving 0.01 g of L-Dopa (from Merck) in water which was diluted to 50 mL with water in a 50-mL volumetric flask. The solution was kept in a refrigerator at 4°C in the dark. More dilute solutions were prepared by serial dilution with buffer solution.

Phosphate buffer solutions (PBS) with pH = 2 were used. A SAMA 500 electrochemical workstation (Sama Instruments, Iran) equipped with a personal computer was used for electrochemical measurements and data analysis. The SAMA software was used for control and data acquisition.

Characterization

The morphology and size of the products were characterized by scanning electron microscopy (SEM; Holland Philips XL30). The crystalline phase was determined by powder x-ray diffraction (XRD) using λ (Cu Kα) = 1.5418 Å. The ultraviolet–visible (UV–vis) absorption spectra were measured on a spectrophotometer (Rayleig). The PL spectra were recorded at room temperature by a 300-nm excitation from an Xe lamp (Avantes/Avaspec 2048).

Synthesis of ZnO, TiO_2 and 1 wt.% Fe-doped ZnO Nanorods and TiO_2 Nanoparticles

All nanostructures were prepared by a hydrothermal method at low temperature without using any template. For preparation of undoped ZnO or TiO_2, 5 mmol $Zn(CH_3COO)_2.2H_2O$ or 5 mmol $TiCl_4$ was dissolved in 50 mL distilled water at 25 ± 1°C with vigorous stirring for 30 min. Then, sodium hydroxide (NaOH) powder was added to the above solution under stirring (10 mmol for the synthesis of ZnO and 25 mL NaOH 1 M for the synthesis of TiO_2). The solution was transferred to an autoclave and kept at 90°C in oven for 2 h. After completion of the reaction, the white product was filtered and washed with distilled water until free from impurities, then dried at room temperature and calcined at 400°C for 2 h.

Samples of 1% Fe-doped ZnO and 1% Fe-doped TiO_2 were prepared by the simple hydrothermal method. Similar to the above method, 5 mmol $Zn(CH_3COO)_2.2H_2O$ in one beaker was dissolved in 25 mL distilled water and 0.05 mmol $FeCl_3$,$6H_2O$ was dissolved in 25 mL distilled water in another beaker under stirring for 30 min at room temperature. Then, the $FeCl_3$ solution was transferred to the first beaker and 10 mmol NaOH was added to the solution and again stirred for 5 min. Next, the solution was transferred to a autoclave, which was sealed and heated to 90°C for 2 h. Finally, the product was calcined at 400°C for 2 h. The sample, after doping with Fe, was named FeZnO.

For the synthesis of 1%Fe-doped TiO_2, firstly, 5 mmol $TiCl_4$ was dissolved in 50 mL distilled water with vigorous stirring for 30 min. Secondly, 25 mL NaOH 1 M was added to the solution and again stirred for 5 min. Thirdly, the solution was transferred to an autoclave, which was sealed and heated to 90°C for 2 h. Finally, the product was calcined at 400°C for 2 h. The sample, after doping with Fe, was named $FeTiO_2$.

Preparation of Modified Electrodes

CPEs were prepared by thoroughly hand-mixing 1 mg of undoped ZnO, undoped TiO_2, Fe-doped ZnO and Fe-doped TiO_2 dispersed in 1 mL ethanol in an ultrasound bath for 30 min to obtain a homogeneous dispersion. Prior to use, a mirror-like surface was obtained by polishing the electrode on a weighing paper. Then 3 μL of the suspension was cast on the CPE surface and dried at room temperature. The resulting electrodes were denoted as ZnO/CPE and TiO_2/CPE. At the same time, 1 mg/mL FeZnO and TiO_2 ethanol suspension solutions were prepared and cast on the CPE surface to obtain FeZnO/CPE and $FeTiO_2$/CPE, respectively, which were used for the comparison.

RESULTS

Characterizations of Undoped ZnO and TiO_2 and Fe-doped ZnO and TiO_2

We used XRD analysis to identify the crystal structure of the undoped ZnO, undoped TiO_2, Fe-doped ZnO and Fe-doped TiO_2 recorded in the range 20°–80°.

Figure 2a shows the XRD patterns of the undoped ZnO and FeZnO samples. Both samples show nine diffraction peaks at 31.83°, 34.49°, 36.32°, 47.62°, 56.71°, 62.96°, 66.40°, 68.00°, and 69.21°, corresponding to the (100), (002), (101), (102), (110), (103), (200), (112) and (201) planes of the wurtzite hexagonal phase of ZnO, respectively.

No reflection characteristics related to Fe or other crystalline can be observed in the pattern, indicating that the Fe ions replace the Zn ions in the lattice of the ZnO crystals due to smaller or similar ionic radii or because the formed crystallites are too small to be detected via XRD.[20]

The average crystallite sizes of ZnO were evaluated by the Scherrer formula (Eq. 1),[21] on the (101) diffraction peak:

$$D = \frac{0.9\lambda}{\beta \cos \theta} \quad (1)$$

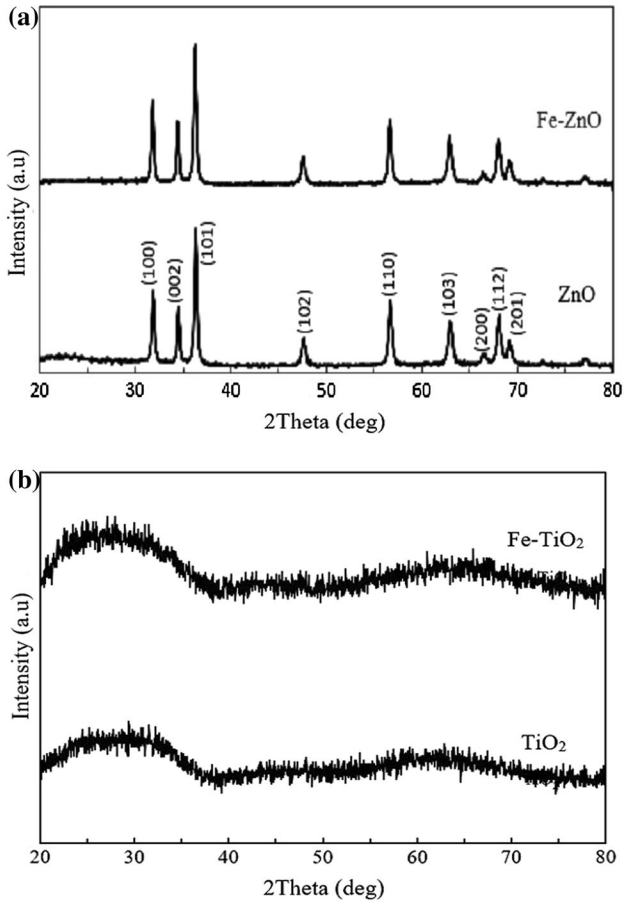

Fig. 2. XRD patterns of (a) ZnO and FeZnO, (b) TiO_2 and $FeTiO_2$ samples.

where D is the crystallite size diameter, θ is the Bragg diffraction angle, λ is the wavelength of the x-ray and β is the full width at half maximum of the diffraction peak. The crystallite sizes are estimated to be 26 nm and 28 nm for ZnO and FeZnO, respectively.

Figure 2b shows the XRD patterns of the TiO_2 and $FeTiO_2$ samples. The flat base lines with very broad XRD peaks of the two samples correspond to the amorphous phase of the samples.

The morphology of the samples was characterized by SEM images as shown in Fig. 3. Figure 3a–d shows granular, nanorods, bone-like and granular morphologies of ZnO, FeZnO, TiO_2 and $FeTiO_2$ structures, respectively. The nanorods morphology reveals that the structure is built up of many granular nanoparticles.

The main reason for these different morphologies is the different ionic radii of the dopants. The Fe-ionic radii is smaller than those of $Zn^{2+}$and Ti^{4+}.[20]

When Zn^{2+} and Ti^{4+} are substituted with Fe ions, the morphology becomes rod-like and granular, respectively. This means that Fe doping may decrease the nucleation rate of FeZnO and $FeTiO_2$ as hydrothermal productions, which is helpful for the regular growth of the FeZnO nanorods and $FeTiO_2$ nanogranular. According to a previous paper, it is reasonable to suggest that Fe doping favors the growth of ZnO rods and TiO_2 granular.[15]

Optical Properties of the Samples

Figure 4 shows the UV–Vis diffuse reflectance spectra of the samples.

The reflectance values were converted to absorbance by application of the Kubelka–Munk function (Eq. 2).[20]

$$\alpha h\nu = A(h\nu - E_g)^{\frac{1}{2}} \quad (2)$$

where α is the absorption coefficient of the material, A is a constant and E_g is the optical band gap energy.

The absorption peak of the ZnO and FeZnO samples are at 387 nm and 420 nm, respectively. The estimated band gap energy of undoped ZnO is ~3.20 eV, while the band gap energy of the Fe-doped ZnO is ~2.95 eV (Fig. 4a).

The absorption peak of the TiO_2 and $FeTiO_2$ samples are at 462 nm and 401 nm, respectively. The estimated band gap energy of undoped TiO_2 is ~3.09 eV, while the band gap energy of the Fe-doped TiO_2 is ~2.68 eV (Fig. 4b).

This result revealed that the doping of Fe ions into ZnO or TiO_2 could shift the optical absorption edge from UV into the visible light range. These red shifts may be due to the charge-transfer transition between the Fe ion d electrons and the conduction or valence band of ZnO or TiO_2.[22,23]

PL is a suitable technique to determine the crystalline quality and the presence of impurities

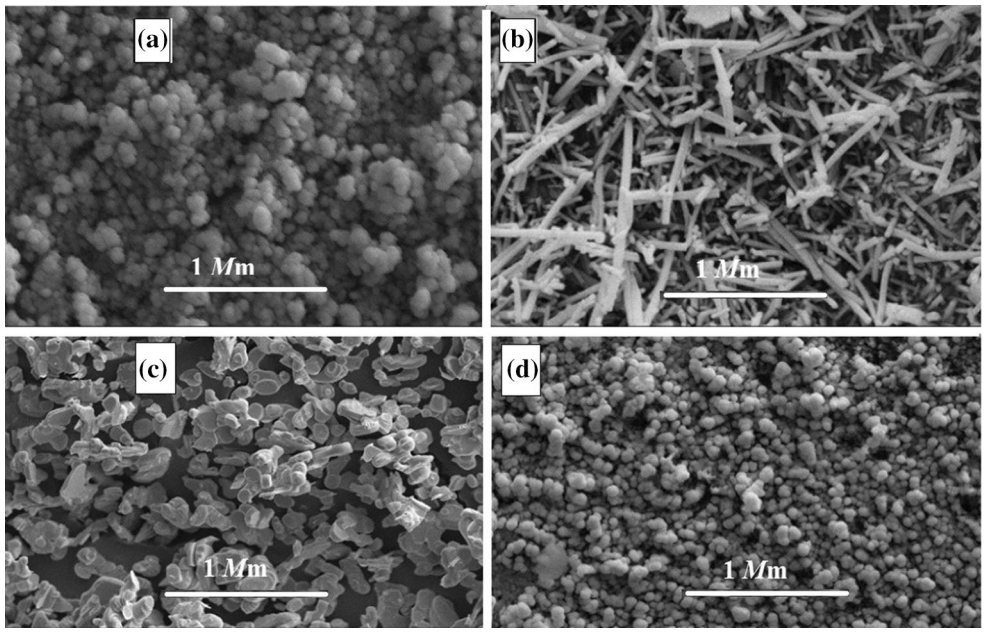

Fig. 3. SEM images of (a) ZnO, (b) FeZnO, (c) TiO_2, (d) $FeTiO_2$ samples.

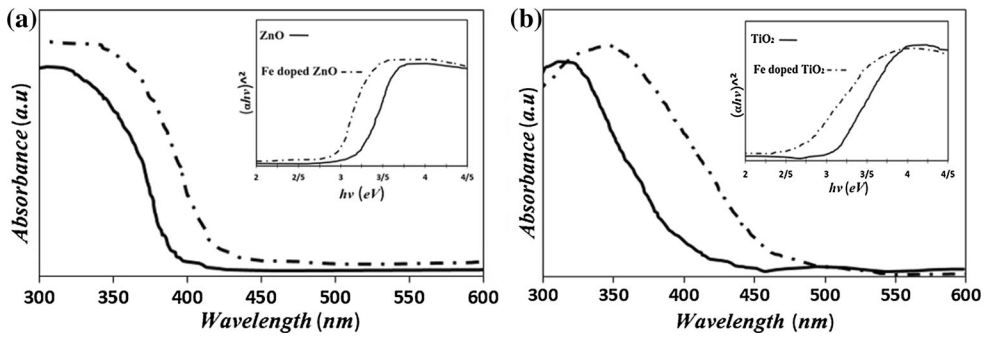

Fig. 4. UV-Vis adsorption and reflectance spectra of the (a) ZnO, FeZnO and (b) TiO_2, $FeTiO_2$ nanostructure samples.

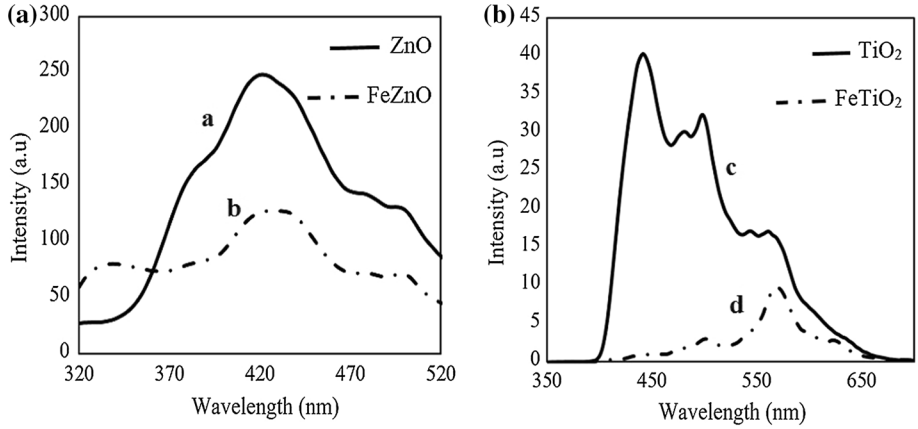

Fig. 5. PL spectra of the (a) ZnO, (b) FeZnO, (c) TiO_2 and (d) $FeTiO_2$ samples with an emission wavelength of 300 nm.

in the materials, as well as exciton fine structures.[24] Figure 5 shows the PL spectra of the undoped and doped samples with an emission wavelength of 300 nm, demonstrating that the band emission intensities decrease with Fe dopant. There is a peak in the range of 370–440 nm that is attributed to the

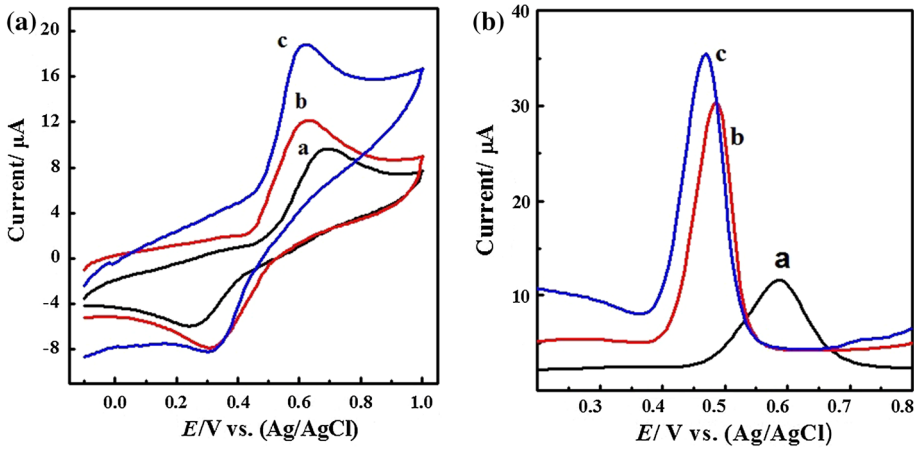

Fig. 6. (a) Cyclic voltammograms and (b) the differential pulse voltammograms of 100 μM L-Dopa on different electrodes. Bare CPE (black line, a) and electrodes modified with ZnO (red line, b) and FeZnO (blue line, c) nano-particles in 0.1 M PBS pH = 2.0 with the potential scan rate of 100 mVs^{-1} and pulse amplitude of 50 mV (Color figure online).

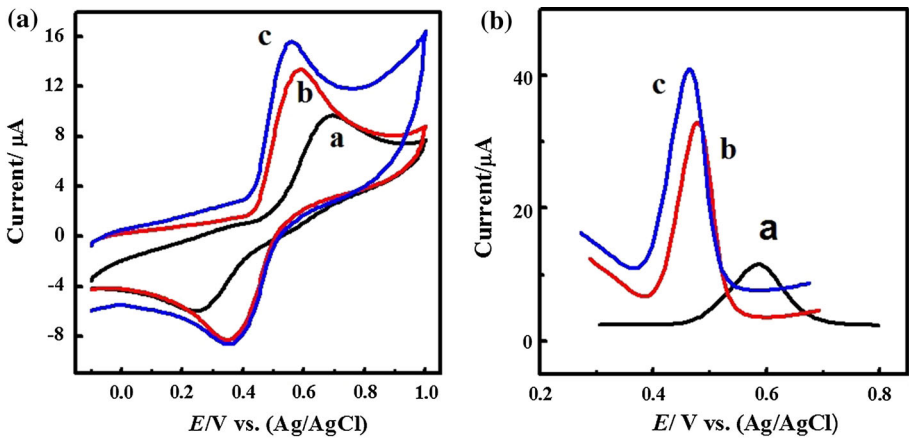

Fig. 7. (a) Cyclic voltammograms and (b) the differential pulse voltammograms of 100 μM L-Dopa on different electrodes. Bare CPE (black line, a) and electrodes modified with TiO_2 (red line, b) and $FeTiO_2$(blue line, c) nano-particles in 0.1 M PBS pH = 2.0 with the potential scan rate 100 mVs^{-1} and pulse amplitude of 50 mV (Color figure online).

Table 1. Cyclic voltammetric (*CV*) and the differential pulse (*DP*) results of 100 μML-Dopa on different modified electrodes

CV						DP	
Electrodes	***I*pc (μA)**	***I*pa(μA)**	***E*pc (V)**	***E*pa(V)**	**ΔEp (V)**	***E*pa(V)**	***I*pa(μA)**
BCPE	−3.88	5.6	263	674	411	584	9.37
ZnO/CPE	−6.7	7.66	323	620	297	483	25.7
TiO_2/CPE	−8.05	8.76	358	578	220	478	27.7
FeZnO/CPE	−7.38	9.79	329	608	279	470	31.5
$FeTiO_2$/CPE	−7.78	9.46	370	549	179	462	33

band edge excitonic luminescence of the undoped and doped ZnO samples.[20]

PLspectra of TiO_2 and $FeTiO_2$ show three peaks at 444 nm, 500 nm, and 567 nm. These visible wavelengths may be attributed to an oxygen deficiency in these samples, such as oxygen vacancies.[24]

Electrochemical Characterizations of the Modified Electrode

The cyclic voltammograms of CPE, ZnO/CPE, TiO_2/CPE, FeZnO/CPE and $FeTiO_2$/CPE in a 0.1-M phosphate buffer solution (pH = 2.0) containing

100 μM L-Dopa were obtained. When the undoped nanostructure samples were added into the CPE, the redox peak currents obviously increased. With adding the FeZnO and $FeTiO_2$ nanostructures into the CPE, a decrease of ΔEp (132 mV and 232 mV) and an increase of the peak current were observed, which could be attributed to the high surface area of FeZnO and $FeTiO_2$, leading to an increase in the electron transfer between the analyte and the electrode surface.

Voltammetric Behavior of L-Dopa

Figures 6 and 7 show the voltammetric responses of 100 μM L-Dopa in 0.1 M PBS (pH = 2.0) on different modified electrodes. No redox peak was observed on modified CPEs in blank PBS, indicating that the modified CPEs were stable in the selected potential region without any redox reaction. The redox peak currents and potentials of L-Dopa on different modified electrodes were recorded and are listed in Table I. It can be seen that a pair of redox peaks appeared on the modified electrodes with the improvement of the voltammetric responses, which was due to the modification of nanomaterials step by step, and the results indicated that the electro-oxidation of L-Dopa had taken place and accelerated on the modified electrodes. Preliminary studies were conducted in order to determine the optimal catalytic activity compared to the electro-oxidation of L-Dopa by the synthesized ZnO and TiO_2 nanoparticles and doped samples with the cyclic and differential pulse voltammetry method. The voltammetric response of L-Dopa was investigated at the surface of an unmodified and a modified CPE with synthesized nanoparticles. Recorded cyclic voltammograms in 0.1 M PBS pH = 2 containing 100 μM L-Dopa with a potential sweep rate of 100 mVs^{-1} are shown in Fig. 6a. At the surface of the CPE, an anodic peak with a peak potential of 674 mV and a cathodic peak with a peak potential of 263 mV for L-Dopa is observed. The potential difference of the oxidation–reduction peaks was found to be equal to 411 mV which expresses its irreversibility at the surface of the unmodified electrode. Oxidation–reduction peak potentials of L-Dopa on CPEs modified with nanoparticles of ZnO and doped ZnO nanoparticles with Few were shifted, respectively, to 620 mV and 608 mV for oxidation and 323 mV and 329 mV for reduction (Fig. 6a). Also, oxidation–reduction peak potentials of L-Dopa on CPEs modified with nanoparticles of TiO_2 and doped TiO_2 nanoparticles with Fe were shifted, respectively, to 578 mV and 549 mV for oxidation and 358 mV and 370 mV for reduction (Fig. 7a).

Notably, results of differential pulse voltammetric (Figs. 6b and 7b) confirmed the results obtained by the CV method. On the other hand, the redox peak currents on the modified electrodes show a significant increase. Based on these observations, it can be concluded that importing modifier nanoparticles indicates an effective catalytic model in the redox reaction of L-Dopa leading to a reduction in overvoltage and a significant increase in redox currents.

Comparison between the electrochemical oxidation of L-Dopa on the surface of two different modified electrodes indicate that the best catalytic activity to reduce the overvoltage of the electrode process and improve sharpness and redox peak current was obtained by a modified electrode with TiO_2 nanoparticles doped with Fe.

CONCLUSION

In the present work, undoped ZnO, undoped TiO_2, 1 wt.% Fe-doped ZnO and 1 wt.% Fe-doped TiO_2 were successfully synthesized by a simple low-temperature hydrothermal method without using any template. The results show that the use of a Fe dopant affects the structural, morphological, photoluminescence (PL), and electrochemical properties of ZnO and TiO_2. The electrochemical behaviors of L-dopa on ZnO/CPE, TiO_2/CPE, FeZnO/CPE and $FeTiO_2$/CPE were carefully investigated with the electrochemical method. The results show that the oxidation peak current of L-dopa obviously increased on $FeTiO_2$/CPE, and high-sensitivity voltammetric responses were obtained.

ACKNOWLEDGEMENT

The authors gratefully acknowledge the financial support of the Research Council of Shahid Rajaee Teacher Training University under contact number 5326.

REFERENCES

1. P. Damier, E.C. Hirsch, Y. Agid, and A.M. Graybiel, *Brain* 122, 1437 (1999).
2. G. Hua, L. Chenb, Y. Guoa, X. Wang, and S. Shao, *Electrochim. Acta* 55, 4711 (2010).
3. T. Yassien, H. Ibrahim, and N. Farhan, *Anal. Methods* 7, 9137 (2015).
4. R.S. Babu, P. Prabhu, and S.S. Narayanan, *J. Nanosci. Nanotech.* 16, 8711 (2016).
5. S.Y. Neto, R.C. Silva Luz, and F.S. Damos, *Electrochem. Commun.* 62, 1 (2016).
6. H. Beitollahi, M. Mazloum-Ardakani, and B. Ganjipour, *H. Naeimi* 24, 362 (2008).
7. M.R. Ganjali, N. Motakef-Kazami, F. Faridbod, S. Khoee, and P. Norouzi, *J. Hazard. Mater.* 173, 415 (2010).
8. M. Mazloum-Ardakani, H. Rajabi, H. Beitollahi, B.F. Mirjalili, A. Akbari, and N. Taghavinia, *Int. J. Electrochem. Sci.* 5, 147 (2010).
9. N. Zhou, J. Wang, T. Chen, Z.G. Yu, and G.X. Li, *Anal. Chem.* 78, 5227 (2006).
10. Y. Zhang, T.R. Nayak, H. Hong, and W. Cai, *Curr. Mol. Med.* 13, 1633 (2013).
11. A.A. Ensafi, H. Bahrami, B. Rezaei, and H.K. Maleh, *Mater. Sci. Eng., C* 33, 831 (2013).
12. H.G. Lin, X.B. Ji, Q.Y. Chen, Y.K. Zhou, C.E. Banks, and K.B. Wu, *Electrochem. Commun.* 11, 1990 (2009).
13. M.H. Mashhadizadeh and E. Afshar, *Electrochim. Acta* 87, 816 (2012).
14. V.K. Gupta, R. Sadeghi, and F. Karimi, *Sens. Act. B Chem.* 186, 603 (2013).
15. M. Meshki, M. Behpour, and S. Masoum, *J. Electroanal. Chem.* 740, 1 (2015).
16. M. Fouladgar, *Measurement* 86, 141 (2016).

17. Y. Wang, J. Chen, C. Zhou, L. Zhou, Y. Kong, H. Long, and S. Zhong, *Electrochim. Acta* 115, 269 (2014).
18. M.M. Ardakani, M.A.S. Mohseni, H. Beitollahi, A. Benvidi, and H. Naeimi, *Chin. Chem. Lett.* 21, 1471 (2010).
19. Y.C. Wang and Y.J. Xu, *J. Huazhong Norm. Univ. (Nat1. Sci.)* 42, 238 (2008).
20. M.H. Darvishnejad, A. Anaraki Firooz, J. Beheshtian, and A.A. Khodadadi, *RSC Adv.* 6, 7838 (2016).
21. R. Abdullah Mirzaie, A. Anaraki Firooz, F. Kamrani, and A.A. Khodadadi, *Solid State Sci.* 26, 9 (2013).
22. N. Venkatachalam, M. Palanichamy, and V. Murugesan, *Mater. Chem. Phys.* 104, 454 (2007).
23. J.C.S. Wu and C.H. Chen, *J. Photochem. Photobiol., A* 163, 509 (2004).
24. K. Vanheusden, W.L. Warren, C.H. Seager, B.E. Gnade, D.R. Tallant, and J.A. Voigt, *J. Appl. Phys.* 79, 7983 (1996).